Biomedical Optics EXPRESS

Surface-modified complex SU-8 microstructures for indirect optical manipulation of single cells

Badri L. Aekbote,[1] Tamás Fekete,[1] Jaroslaw Jacak,[2] Gaszton Vizsnyiczai,[1] Pál Ormos,[1] and Lóránd Kelemen[1,*]

[1] *Biological Research Centre of the Hungarian Academy of Sciences, Temesvári krt. 62, Szeged 6726, Hungary*
[2] *University of Applied Sciences Upper Austria, Garnisonstraße 21, 4020 Linz, Austria*
**kelemen.lorand@brc.mta.hu*

Abstract: We introduce a method that combines two-photon polymerization (TPP) and surface functionalization to enable the indirect optical manipulation of live cells. TPP-made 3D microstructures were coated specifically with a multilayer of the protein streptavidin and non-specifically with IgG antibody using polyethylene glycol diamine as a linker molecule. Protein density on their surfaces was quantified for various coating methods. The streptavidin-coated structures were shown to attach to biotinated cells reproducibly. We performed basic indirect optical micromanipulation tasks with attached structure-cell couples using complex structures and a multi-focus optical trap. The use of such extended manipulators for indirect optical trapping ensures to keep a safe distance between the trapping beams and the sensitive cell and enables their 6 degrees of freedom actuation.

OCIS codes: (140.7090) Ultrafast lasers; (160.1435) Biomaterials; (160.5470) Polymers; (180.2520) Fluorescence microscopy; (230.4000) Microstructure fabrication; (230.6120) Spatial light modulators; (310.0310) Thin films; (350.3390) Laser materials processing; (350.4855) Optical tweezers or optical manipulation.

References and links

1. J. Nilsson, M. Evander, B. Hammarström, and T. Laurell, "Review of cell and particle trapping in microfluidic systems," Anal. Chim. Acta **649**(2), 141–157 (2009).
2. L. Amato, Y. Gu, N. Bellini, S. M. Eaton, G. Cerullo, and R. Osellame, "Integrated three-dimensional filter separates nanoscale from microscale elements in a microfluidic chip," Lab Chip **12**(6), 1135–1142 (2012).
3. D. R. Gossett, W. M. Weaver, A. J. Mach, S. C. Hur, H. T. K. Tse, W. Lee, H. Amini, and D. Di Carlo, "Label-free cell separation and sorting in microfluidic systems," Anal. Bioanal. Chem. **397**(8), 3249–3267 (2010).
4. J. Wong, A. Chilkoti, and V. T. Moy, "Direct force measurements of the streptavidin-biotin interaction," Biomol. Eng. **16**(1-4), 45–55 (1999).
5. J. Helenius, C.-P. Heisenberg, H. E. Gaub, and D. J. Muller, "Single-cell force spectroscopy," J. Cell Sci. **121**(11), 1785–1791 (2008).
6. O. Guillaume-Gentil, E. Potthoff, D. Ossola, C. M. Franz, T. Zambelli, and J. A. Vorholt, "Force-controlled manipulation of single cells: from AFM to FluidFM," Trends Biotechnol. **32**(7), 381–388 (2014).
7. E. A. Abbondanzieri, W. J. Greenleaf, J. W. Shaevitz, R. Landick, and S. M. Block, "Direct observation of base-pair stepping by RNA polymerase," Nature **438**(7067), 460–465 (2005).
8. J.-C. Meiners and S. R. Quake, "Femtonewton force spectroscopy of single extended DNA molecules," Phys. Rev. Lett. **84**(21), 5014–5017 (2000).
9. K. Bambardekar, R. Clément, O. Blanc, C. Chardès, and P.-F. Lenne, "Direct laser manipulation reveals the mechanics of cell contacts in vivo," Proc. Natl. Acad. Sci. U.S.A. **112**(5), 1416–1421 (2015).
10. L. Oroszi, P. Galajda, H. Kirei, S. Bottka, and P. Ormos, "Direct measurement of torque in an optical trap and its application to double-strand DNA," Phys. Rev. Lett. **97**(5), 058301 (2006).
11. P. R. T. Jess, V. Garcés-Chávez, D. Smith, M. Mazilu, L. Paterson, A. Riches, C. S. Herrington, W. Sibbett, and K. Dholakia, "Dual beam fibre trap for Raman micro-spectroscopy of single cells," Opt. Express **14**(12), 5779–5791 (2006).
12. D. Wolfson, M. Steck, M. Persson, G. McNerney, A. Popovich, M. Goksör, and T. Huser, "Rapid 3D fluorescence imaging of individual optically trapped living immune cells," J. Biophotonics **8**(3), 208–216 (2015).
13. S. Rao, S. Raj, S. Balint, C. B. Fons, S. Campoy, M. Llagostera, and D. Petrov, "Single DNA molecule detection in an optical trap using surface-enhanced Raman scattering," Appl. Phys. Lett. **96**(21), 213701 (2010).

#252006 Received 20 Oct 2015; revised 19 Nov 2015; accepted 20 Nov 2015; published 7 Dec 2015

14. N. Maghelli and I. M. Tolić-Nørrelykke, "Versatile laser-based cell manipulator," J. Biophotonics **1**(4), 299–309 (2008).
15. E. Bertseva, D. Grebenkov, P. Schmidhauser, S. Gribkova, S. Jeney, and L. Forró, "Optical trapping microrheology in cultured human cells," Eur Phys J E Soft Matter **35**(7), 63 (2012).
16. H. Zhang and K.-K. Liu, "Optical tweezers for single cells," J. R. Soc. Interface **5**(24), 671–690 (2008).
17. N. McAlinden, D. G. Glass, O. R. Millington, and A. J. Wright, "Accurate position tracking of optically trapped live cells," Biomed. Opt. Express **5**(4), 1026–1037 (2014).
18. Y. Liu, D. K. Cheng, G. J. Sonek, M. W. Berns, C. F. Chapman, and B. J. Tromberg, "Evidence for localized cell heating induced by infrared optical tweezers," Biophys. J. **68**(5), 2137–2144 (1995).
19. S. Ayano, Y. Wakamoto, S. Yamashita, and K. Yasuda, "Quantitative measurement of damage caused by 1064-nm wavelength optical trapping of Escherichia coli cells using on-chip single cell cultivation system," Biochem. Biophys. Res. Commun. **350**(3), 678–684 (2006).
20. M. B. Rasmussen, L. B. Oddershede, and H. Siegumfeldt, "Optical tweezers cause physiological damage to Escherichia coli and Listeria bacteria," Appl. Environ. Microbiol. **74**(8), 2441–2446 (2008).
21. H. Liang, K. T. Vu, P. Krishnan, T. C. Trang, D. Shin, S. Kimel, and M. W. Berns, "Wavelength dependence of cell cloning efficiency after optical trapping," Biophys. J. **70**(3), 1529–1533 (1996).
22. G. Leitz, E. Fällman, S. Tuck, and O. Axner, "Stress response in *Caenorhabditis elegans* caused by optical tweezers: wavelength, power, and time dependence," Biophys. J. **82**(4), 2224–2231 (2002).
23. A. Thakur, S. Chowdhury, P. Švec, C. Wang, W. Losert, and S. K. Gupta, "Indirect pushing based automated micromanipulation of biological cells using optical tweezers," Int. J. Robot. Res. **33**(8), 1098–1111 (2014).
24. D. B. Phillips, J. A. Grieve, S. N. Olof, S. J. Kocher, R. Bowman, M. J. Padgett, M. J. Miles, and D. M. Carberry, "Surface imaging using holographic optical tweezers," Nanotechnology **22**(28), 285503 (2011).
25. S. Kawata, H. B. Sun, T. Tanaka, and K. Takada, "Finer features for functional microdevices," Nature **412**(6848), 697–698 (2001).
26. D. B. Phillips, S. H. Simpson, J. A. Grieve, R. Bowman, G. M. Gibson, M. J. Padgett, J. G. Rarity, S. Hanna, M. J. Miles, and D. M. Carberry, "Force sensing with a shaped dielectric micro-tool," Europhys. Lett. **99**(5), 58004 (2012).
27. D. Palima, A. R. Bañas, G. Vizsnyiczai, L. Kelemen, P. Ormos, and J. Glückstad, "Wave-guided optical waveguides," Opt. Express **20**(3), 2004–2014 (2012).
28. V. Melissinaki, M. Farsari, and S. Pissadakis, "A Fiber-Endface, Fabry–Perot Vapor Microsensor Fabricated by Multiphoton Polymerization," J. Select. Top. Quantum Electr. **21**, 5600110 (2015).
29. H. Hidai, H. Jeon, D. J. Hwang, and C. P. Grigoropoulos, "Self-standing aligned fiber scaffold fabrication by two photon photopolymerization," Biomed. Microdevices **11**(3), 643–652 (2009).
30. A. Selimisa, V. Mironovb, and M. Farsari, "Direct laser writing: Principles and materials for scaffold 3D printing," Microelectron. Eng. **132**, 83–89 (2015).
31. F. Formanek, N. Takeyasu, T. Tanaka, K. Chiyoda, A. Ishikawa, and S. Kawata, "Three-dimensional fabrication of metallic nanostructures over large areas by two-photon polymerization," Opt. Express **14**(2), 800–809 (2006).
32. T. Ikegami, R. Ozawa, M. P. Stocker, K. Monaco, J. T. Fourkas, and S. Maruo, "Development of optically-driven metallic microrotors using two-photon microfabrication," J. Laser Micro/Nanoeng. **8**(1), 6–10 (2013).
33. M. Farsari, G. Filippidis, T. S. Drakakis, K. Sambani, S. Georgiou, G. Papadakis, E. Gizeli, and C. Fotakis, "Three-dimensional biomolecule patterning," Appl. Surf. Sci. **253**(19), 8115–8118 (2007).
34. Y. L. Sun, Q. Li, S. M. Sun, J. C. Huang, B. Y. Zheng, Q. D. Chen, Z. Z. Shao, and H. B. Sun, "Aqueous multiphoton lithography with multifunctional silk-centred bio-resists," Nat. Commun. **6**, 8612 (2015).
35. B. L. Aekbote, J. Jacak, G. J. Schütz, E. Csányi, Zs. Szegletes, P. Ormos, and L. Kelemen, "Aminosilane-based functionalization of two-photon polymerized 3D SU-8 microstructures," Eur. Polym. J. **48**(10), 1745–1754 (2012).
36. B. L. Aekbote, F. Schubert, P. Ormos, and L. Kelemen, "Gold nanoparticle-mediated fluorescence enhancement by two-photon polymerized 3D microstructures," Opt. Mater. **38**, 301–309 (2014).
37. G. Vizsnyiczai, L. Kelemen, and P. Ormos, "Holographic multi-focus 3D two-photon polymerization with real-time calculated holograms," Opt. Express **22**(20), 24217–24223 (2014).
38. Y. Wang, J. H. Pai, H. H. Lai, C. E. Sims, M. Bachman, G. P. Li, and N. L. Albritton, "Surface graft polymerization of SU-8 for bio-MEMS applications," J. Micromech. Microeng. **17**(7), 1371–1380 (2007).
39. R. Schlapak, P. Pammer, D. Armitage, R. Zhu, P. Hinterdorfer, M. Vaupel, T. Frühwirth, and S. Howorka, "Glass surfaces grafted with high-density poly(ethylene glycol) as substrates for DNA oligonucleotide microarrays," Langmuir **22**(1), 277–285 (2006).
40. J. Satulovsky, M. A. Carignano, and I. Szleifer, "Kinetic and thermodynamic control of protein adsorption," Proc. Natl. Acad. Sci. U.S.A. **97**(16), 9037–9041 (2000).
41. K. L. Prime and G. M. Whiteside, "Adsorption of proteins onto surfaces containing end-attached oligo (ethylene oxide): a model system using self-assembled monolayers," J. Am. Chem. Soc. **115**(23), 10714–10721 (1993).
42. J. Hesse, M. Sonnleitner, A. Sonnleitner, G. Freudenthaler, J. Jacak, O. Höglinger, H. Schindler, and G. J. Schütz, "Single-molecule reader for high-throughput bioanalysis," Anal. Chem. **76**(19), 5960–5964 (2004).
43. R. Di Leonardo, A. Búzás, L. Kelemen, G. Vizsnyiczai, L. Oroszi, and P. Ormos, "Hydrodynamic synchronization of light driven microrotors," Phys. Rev. Lett. **109**(3), 034104 (2012).

#252006 Received 20 Oct 2015; revised 19 Nov 2015; accepted 20 Nov 2015; published 7 Dec 2015

1. Introduction

Mechanical manipulation of micrometer and nanometer scale biological objects has become a significant issue in the bio-nanotechnology field during the last decade. The wide variety of objects in terms of complexity and size forced the development of 2D and 3D micromanipulation techniques that include transfer, trapping [1], separation [2], collection [3], measurement of interaction forces [4,5] or even microsurgery or micro-infusion [6]. Among several competing 3D micromanipulation techniques, optical tweezers (OT) is one method with the great advantage of being practically non-invasive. OT has proved its applicability in biology by measuring displacement with sub-nanometer accuracy [7], forces with femtoNewton sensitivity [8], cell or DNA mechanics [9,10] or by helping collect spectroscopic information on cells [11,12] or DNA [13].

One can classify the nature of the OT manipulation of biological objects distinguishing direct and indirect interaction. OT can directly manipulate cell organelles [14], study the elasticity of cell interior [15] or manipulate and image even entire cells [16,17]. Indirect manipulation becomes necessary, for instance, in case of biological macromolecules which themselves cannot be trapped. A further important motivation for indirect manipulation is to avoid photo- or thermal damage the intense optical field may impose on the sensitive biological matter, cells in particular [18–20]. Although with careful choice of the wavelength, power and exposure time one can reduce this effect [21,22] intermediate objects, such as chemically functionalized microbeads [7] or other cells [23] can be often found between the cell to be manipulated and the optical trap. While the use of microbeads is well-established, it is limited to motions only with 3 degrees of freedom and it still brings the trapping field close to the trapped object. To overcome these limitations, the use of extended, specifically designed intermediate objects is a promising alternative.

The two key requirements for such an intermediate object is the six degrees of freedom motion (rotation and translation) and providing a safe distance between the object of study and the intense light in the focus of the optical trap. These two added features have already attracted the attention of the optical micromanipulation community. Recently, trapped rod-shaped microorganisms, diatoms were characterized as possible intermediate tools to study biological samples [24]. It is also the result of the recent past that the technique of two-photon polymerization (TPP) [25] was used to prepare artificial microtools for OT applications with highly task-specific shape [26,27]. These polymerized structures are designed to have two functional parts separated even by micrometers: the handle part that interacts with the optical field and the probe part that performs the main function of the tool (scanning a surface or emitting light). The great advantage of TPP is that tailor-made probes can be prepared practically in one step with on-demand handle arrangement and probe shape. With respect to optical trapping, there's also great potential for the use of TPP not only to make structures to be trapped but to create integrated micro-optical elements into existing optical systems [28] where these elements might even shape the trapping beam itself.

However, in order to use trapped microstructures effectively for biological tasks, they need to be functionalized. Coated TPP structures have primarily been used for cell culture experiments [29,30] but selective metallization [31,32], or selective protein coating using photobiotin linker [33] have also been demonstrated. Recently Sun and associates used femtosecond laser direct writing to develop a single step procedure to fabricate multifunctional metal/bio-macromolecule complex micro/nanodevice elements for mechanical and electrical applications [34] eliminating the need for further functionalization. Previously we showed aminosilane-based functionalization of polymerized microtools with the protein streptavidin for optical trap actuation [35]. However, the binding efficiency of these microtools to live cells was not yet experimentally investigated. We also recently showed the ability of TPP structures to enhance fluorescence when densely coated with gold nanoparticles [36].

#252006 Received 20 Oct 2015; revised 19 Nov 2015; accepted 20 Nov 2015; published 7 Dec 2015

In this paper we show that 3D microstructures made of SU-8 photopolymer by TPP can be functionalized effectively and specifically in order to use for indirect optical micromanipulation of single cells. We show that using polyethylene glycol diamine (PEG-diamine) as a linker between the microtools and the protein layer assembled on their surfaces provides high enough protein density for a fast microstructure-cell attachment. This linker molecule provided more than four times higher protein density than APTES which was used in our previous work. In this work we used not only biotin to specifically link streptavidin to the SU-8 microstructures but also studied the use of glutaraldehyde to non-specifically link proteins to them; we also quantified the protein surface densities provided by the different coating procedures. Most importantly, for the first time, the functionalized TPP microstructures were optically trapped and tested for their binding efficiency towards single cells. Basic indirect optical cell micromanipulation tasks were also demonstrated using extended structures held by multiple optical traps.

2. Materials and methods

The SU-8 2002 and 2007 photoresist and SU-8 developer (mr-Dev 600) were purchased from Micro Resist Technology GmbH (Germany), glass slides (20x20 mm and 24x40 mm) from Menzel Glaser (Germany). Poly(ethylene glycol)bis(amine) (PEG-diamine) (2000 MW, cat. No. 14501), ceric-ammonium nitrate (CAN) (cat. No.: 22249), bovine serum albumin (BSA) (cat. no. A7906) and Tween 20 (cat. no. P9416) were purchased from Sigma-Aldrich and glutaraldehyde (cat. no. A17876) from Alfa Aesar. DyLight 649 fluorophore-conjugated streptavidin (prod no. 35515, λ_{exc} = 646 nm, λ_{em} = 674 nm), Alexa568-conjugated IgG, goat, anti-rabbit antibody (cat. no. A-11004), and EZ-Link Sulfo-NHS-Biotin (cat. no. 21217) was purchased from Thermo Fisher Scientific Inc., USA. Nitric acid, isopropanol and ethanol are from Molar Chemical KFT, (Budapest). Deionized water (18 MΩcm) was produced by a Synergy UV system (Millipore, USA). HEPES buffer was prepared in-house containing 5 mM HEPES (4-(2-Hydroxyethyl)piperazine-1-ethanesulfonic acid), 150 mM NaCl, 5.2 mM KCl, 2.2 mM $CaCl_2$, 0.2 mM $MgCl_2.6H_2O$, 6 mM $NaHCO_3$ and 2.8 mM D-glucose.

2.1 Fabrication of SU-8 layers and microstructures

The efficiency of the functionalization protocol was tested on large area SU-8 surfaces made by UV lithography as well as on two-photon polymerized microblocks similarly to our previous approach [35]. The UV polymerization took place on glass microscope cover slides, using 2-3 μm thick SU-8 layers and UV illumination with the 365 nm line of a mercury lamp (dose: 340 mJ/cm^2). All the two-photon polymerized SU-8 microstructures were made of SU-8 2007 with the system described elsewhere [37]. Shortly, the beam of an ultrashort-pulsed laser (C-Fiber A, Menlo Systems, λ = 795 μm, 100 fs pulses, 100 MHz repetition rate) was focused into a 20 μm thin photoresist layer supported by a microscope cover slide. The 3D scanning of the focus in the layer was carried out by a piezo stage. The illuminated SU-8 layers were processed with a standard protocol: post-bake at 95 °C for 10 mins, development in mrDev 600, rinsing in ethanol and drying with a stream of nitrogen.

#252006 Received 20 Oct 2015; revised 19 Nov 2015; accepted 20 Nov 2015; published 7 Dec 2015

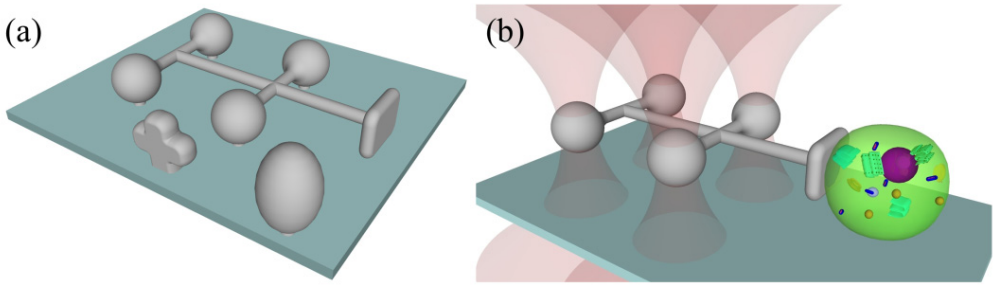

Fig. 1. a) Drawing of microstructures polymerized onto a glass substrate for cell adhesion experiments: cross, ellipsoid and four-spheroid manipulator. b) Scheme of the indirect trapping of a cell with a four-spheroid manipulator. The four static trapping beams are arranged on the centers of the spheroids with holographic optical tweezers.

For the protein surface-density quantification experiments microblocks were two-photon polymerized with the size of 15 μm x 15 μm x 6 μm with a 63 × Zeiss LD Plan-Neofluar focusing objective (NA = 0.75); the laser power was 8 mW and the scan speed 40 μm/s. For the optical trapping experiments various, substrate-attached microstructures were polymerized (Fig. 1) but this time the objective was a Zeiss Achroplan, 100 × oil immersion one (NA 1.25). These structures were the following (Fig. 1(a)): ellipsoids with 6 μm large axis and 4 μm small axis and crosses with 6 μm arms and complex optical tools. This latter structure consisted of four spheroids of 4 μm diameter as handles, a plate of 3 x 4 μm as the probe part situating 10 μm away from the nearest spheroid and their connecting rods. The applied laser power was 3 mW and the scan speed was between 1 μm/s and 40 μm/s.

2.2 Protein coating of SU-8

The methods described below were applied on the SU-8 structures in order to bind streptavidin and IgG to them. The process is similar as reported earlier the main differences being the use of *i)* PEG-diamine as an amine-terminated linker molecule and *ii)* glutaraldehyde as a nonspecific protein crosslinker. In the first method detailed below we utilize the high-affinity biotin-streptavidin linkage to bind this protein specifically while in the second one we replace biotin with glutaraldehyde to allow practically any protein to be bound to the structures.

First, the SU-8 structures are incubated in the mixture of 1 M nitric acid and 0.1 M CAN for 30mins, at room temperature (RT) in both methods to create hydroxyl groups on the surface [35,38]. The rinsed and dried structures were then treated with PEG-diamine of MW 2000 dissolved in methanol (15 mM) [39]; this length have been shown to resist nonspecific biomolecule adsorption [40,41]. Then the slides were incubated on a hot plate for 20 mins at 60 °C, cooled to RT, rinsed in ultrapure water thoroughly and finally dried under a stream of nitrogen. At his point the two methods branched. We used sulfo-NHS biotin as a specific streptavidin linker in the first one. Sulfo-NHS biotin, freshly dissolved to 1 mg/mL in phosphate-buffered saline (PBS) (pH 7.4) was reacted with the PEG-diamine treated SU-8 structures for 4 hrs at RT. The sample was then washed with PBS twice for 10 mins to remove unbound biotin and immediately used for streptavidin incubation. Streptavidin functionalization was done using unconjugated protein or its DyLight 649 fluorophore conjugated version. We chose this fluorophore to avoid the autofluorescence region of SU-8. The biotinated SU-8 structures were incubated in 10 nM streptavidin dissolved in PBS overnight at RT. Finally, we washed the sample thoroughly with 0.05% aqueous solution of Tween 20, then with 1% BSA solution and lastly with PBS (10 mins each) to remove any unbound streptavidin.

In the other branch of the protein coating the PEG-diamine treated SU-8 samples were incubated in 2.5% glutaraldehyde solution in PBS for 90 mins at RT. The samples were then

#252006 Received 20 Oct 2015; revised 19 Nov 2015; accepted 20 Nov 2015; published 7 Dec 2015

rinsed with ultrapure water to remove unbound glutaraldehyde. To bind the protein to the surface, the samples were incubated in 10 nM solutions of DyLight 649-conjugated streptavidin or in 7 nM Alexa 568-conjugated IgG overnight at RT. Finally the samples were rinsed and kept in PBS until use.

For the trapping efficiency measurements with the ellipsoids and crosses and the indirect manipulation experiments with the complex 3D microtools the structures were coated specifically with non-fluorescent streptavidin linked with sulfo-NHS biotin. The streptavidin coated structures were immersed into 3 mL HEPES buffer containing 1% BSA and removed from the surface mechanically under visual observation on a brightfield microscope. The freely floating structures were then collected into a tapered capillary tube together with about 3 μL solution from which they were eventually injected into the reservoir containing the cells.

The efficiency of the coating protocols in terms of protein surface density over the SU-8 surfaces and the adjacent glass substrate was tested by the same single molecule scanner built on a Zeiss 200M microscope (Zeiss, Oberkochen, Germany) that was used in our previous works [35,42]. Shortly, the fluorescent streptavidin-coated surfaces were illuminated by a Kr + laser (λ = 647 nm, Innova 301, Coherent, Santa Clara, USA) and the IgG-coated ones by a Ar-laser at 514 nm. The fluorescence was collected onto a back-illuminated CCD camera (NTE/CCD-1340/100-EMB, 20 μm pixel size, Roper Scientific, Trenton, USA) by a 100x/NA = 1.45 oil immersion objective (α Plan-Fluar, Zeiss). The sample was scanned at 0.137 kW/cm^2 and 0.097 kW/cm^2 excitation power for DyLight 649 and Alexa 568, respectively and illuminated for 200 ms in all measurements. During the process, first the signal from single streptavidin molecules was recorded with a diluted solution of the protein and the average peak intensity and peak area were determined for these molecules by Gaussian fitting. Then, after recording a fluorescent image of the streptavidin-coated surface, the result of this fitting was used to calculate the amount of surface-bound protein, taking into account the average number of fluorophores on each streptavidin.

2.3 Functionalization of K562 cells with biotin

We used the K562 cell line in our trapping experiments. In order to attach them to the functionalized microtools the cells needed to be biotinated. The protocol recommended by the supplier was followed with minor changes: 1 mL of the cultivated cells (approx. 6*10^5 cells) were centrifuged three times at 4 °C at 1700 RPM (RCF: 300) for 2 mins, where after each centrifuging the supernatant was carefully replaced with fresh ice cold HEPES buffer and gently mixed. After the last removal of the supernatant sulfo-NHS biotin freshly dissolved in cold HEPES buffer to 2 mg/mL concentration was added to the cells, gently mixed and incubated on ice for 30 mins. Next, the suspension was centrifuged as before and the supernatant was replaced by HEPES to wash out sulfo-NHS biotin; this step was repeated twice. Finally, the supernatant was replaced twice with HEPES containing 1% BSA, leaving a final volume of ~300 μL cell suspension.

Approximately 60 μL of the biotinated cell suspension were injected into a reservoir (Secure-Seal Hybridization chamber, S24733, Thermo Fisher Scientific, USA) that has a glass cover slip bottom. Then the collected functionalized polymer microstructures carried by ~3 μL HEPES were added to the cell suspension. Approximately 20-40% of the cells remained floating during the first 1hour of the subsequent trapping experiments, the rest were attached to the bottom of the chamber. The attachment of the TPP structures to the cells were tested on both the attached and the free ones, but optical manipulation could obviously be performed only on the free ones.

2.4 Indirect optical trapping of cells

The main goal of this paper is to show that two-photon polymerized microtools can be functionalized effectively in order to be used for indirect trapping and manipulation of single cells. We demonstrated this on an optical tweezers system previously used in DiLeonardo et

#252006 Received 20 Oct 2015; revised 19 Nov 2015; accepted 20 Nov 2015; published 7 Dec 2015

al [43]. It is a holographic optical trap (HOT) system built on a Zeiss Axio Observer A1 inverted microscope with a continuous wave fiber laser (λ = 1070 nm, IPG-YLM-10, IPG Photonics) as a light source, an Olympus UPlanSApo water immersion objective (60X, NA = 1.2) as a focusing element, a motorized microscope stage (Märzhäuser, Germany) for sample translation and a spatial light modulator (PLUTO NIR, Holoeye, Germany) to generate multiple traps. The total optical power at the entrance of the objective pupil was 125 mW when using ellipsoids and crosses and 175 mW for the complex cell manipulator structures. The optical path included a half wave plate to rotate the orientation of the plane of polarization of the beam in order to orient the trapped, protein-coated crosses. The holographic traps were kept static in all the manipulation experiments and only the sample was translated with respect to them.

In order to clarify the necessity of the functionalization and to determine the binding efficiency of the functionalized TPP structures to the cells we performed several attachment tests trapping the crosses or ellipsoids with steady traps. These structures approached the cells by moving the sample stage and were pushed against them for not more than 2 s. We did not specifically control the speed of approach, which was approximately 0.5-1 μm/s. Then the stage was retracted and checked if the structure remained attached to the cells. These tests were performed with four combinations of cell and microstructure functionalization presented in Table 1.

A lower limit for the binding strength between the cell and the microstructure was given by performing a viscous drag experiment when a cell-attached ellipsoid was trapped and the couple was translated with a known speed relative to the medium. Approximating the cell with a sphere, the drag force acting on it due to viscosity can be calculated by the equation $F_d = 6\pi\mu Rv$, where μ is the viscosity of water, R is the radius of the cell and v is the speed of the translation. As long as the couple remains in the trap during the translation and does not separate, the calculated viscous force that acts on the cell is smaller than the binding force that keeps the couple together. The application of crosses for the attachment test shows the advantage of the use of complex TPP structure for indirect trapping. Due to their planar shape, the direction of the crosses could be aligned by changing the polarization direction with the half wave plate [10]; this way they could touch the cell either with the end of their arms or with their flat part, presenting interaction areas of different size. Eventually, we also used the structure with four spheroids to indirectly trap and translate cells within the sample chamber. After the structure was trapped with a set of four static optical traps generated in the HOT (for trapping beam arrangement see Fig. 1(b)), a cell was approached with the flat probe part and attached. Next, the sample chamber was translated along all three directions at constant speed and the position of the cell-structure couple was evaluated by video microscopy.

3. Results and discussion

3.1 Protein density on SU-8 surfaces

The protein surface density was quantified at various stages of the different functionalization protocols. The graphs on Fig. 2 show the surface densities measured on pristine UV-polymerized layers as well as on fully functionalized UV-polymerized layers and TPP microblocks using the biotin-based (Fig. 2(a)) and the glutaraldehyde-based (Fig. 2(b)) protocol. First of all, both graphs show that the linker layers highly increase protein binding for both methods: the biotinated SU-8 surface binds about 500 times more streptavidin than the pristine one, whereas this number is 20-100 for the glutaraldehyde-based method. In the case of specific streptavidin binding there is no significant difference between the UV- and the TPP polymerized SU-8 surface, both reaching about $4 \cdot 10^4$ molecules/μm^2 density.

#252006 Received 20 Oct 2015; revised 19 Nov 2015; accepted 20 Nov 2015; published 7 Dec 2015

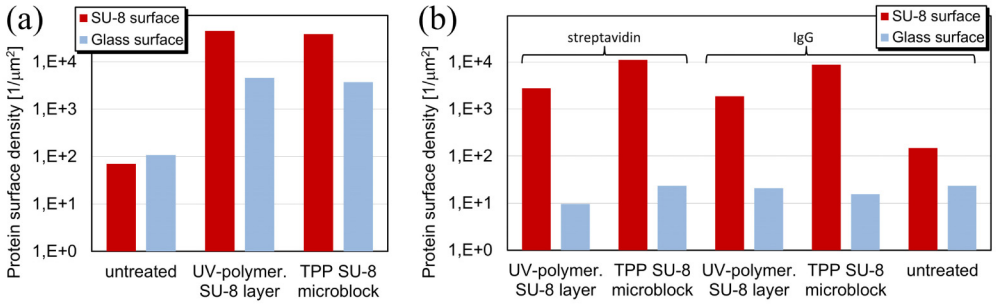

Fig. 2. Surface densities of protein layers obtained on SU-8 surfaces. a) Protein surface density obtained with the specific streptavidin coating method and measured on untreated and biotinated SU-8 and glass surfaces. b) Streptavidin and IgG surface densities measured on glutaraldehyde-treated and untreated SU-8 and glass surfaces (non-specific method).

However, with glutaraldehyde linker the TPP structures were covered with both proteins with about 10^4 molecules/µm^2; this was about 5 times more than for the UV-polymerized layers. We note here that the use of APTES in our previous work [35] instead of PEG-diamine to bind streptavidin specifically (i.e. with sulfo-NHS biotin) resulted in the same density level what was obtained now with glutaraldehyde. Furthermore, with glutaraldehyde we found no significant difference between the surface density of the two kinds of proteins (streptavidin and IgG) which is attributed to the non-specific nature of this linkage. We also observed that there's a selectivity of the protein binding towards the SU-8 surface: in case of biotin-assisted binding about 10 times more protein is found on the SU-8 than on the substrate, whereas using glutaraldehyde there is 100-500 times more protein on the SU-8 than on the glass.

Most importantly for practical purposes, the specific biotin-assisted linkage of streptavidin gives about 4 times higher density than the non-specific method. The figure of $4 \cdot 10^4$ molecules/µm^2 means that there's almost two layers of protein over the surface (considering an ~5 nm diameter for a single streptavidin molecule), ensuring high probability of linkage of the cells to the polymerized structures. We also note that when any of the functionalization steps was missing, significantly lower protein density was observed (data not shown). In Fig. 3(a) and 3(b) bright-field and fluorescent microscopic images of crosses functionalized specifically with DyLight 649-conjugated streptavidin with the highest density and used for cell-attachment are shown, displaying high fluorescence intensity relative to its glass substrate. The complex structures with four spheroids, although with a different probe type, were also successfully functionalized, as shown on Fig. 3(c).

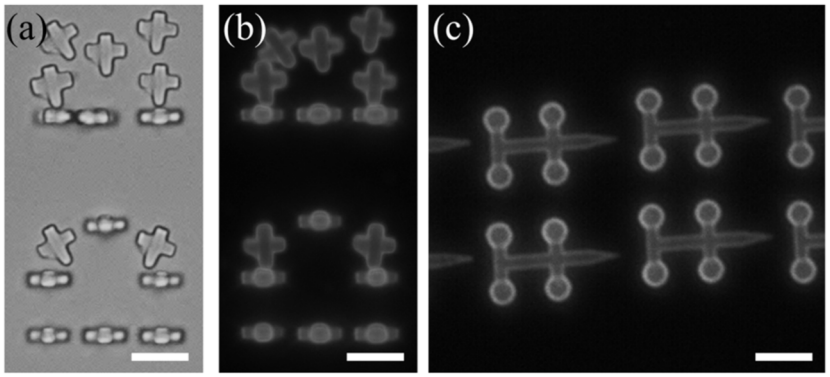

Fig. 3. Optical microscopy images of polymerized structures made for indirect cell trapping. Brightfield (a) and fluorescence (b) microscopy images of crosses and fluorescence image of four-spheroids manipulators (c) coated with fluorescent streptavidin. The structures are still attached onto their substrates, except some of the crosses. Scale bar: 10 µm.

#252006 Received 20 Oct 2015; revised 19 Nov 2015; accepted 20 Nov 2015; published 7 Dec 2015

3.2 Binding efficiency of cells to TPP structures

For the efficient indirect trapping of the cells with TPP structures it is crucial to achieve strong linkage in a reproducible way that also forms fast between the two components. We performed attachment tests on the cells with various functionalization combinations. The primary structures we used were crosses which served two purposes: one was to illustrate that cells can be manipulated with structures that are more complex than the classic microbeads and that they can display contact areas of different size towards the cells. The target cells were selected randomly, being either freely floating or substrate-attached. Figure 4(a)-4(f) shows a series of snapshots of the approach, attachment and translation of a freely floating cell with a trapped cross structure (also see Visualization 1). We regarded the attachment successful if the trap could not remove the structure from the cell surface any more. For substrate-attached cells it meant that the structure was removed from the trap and for freely floating ones the cell was dragged along when the environment was translated. We have to mention here that in some cases when the retraction was slow we could pull a tether from the membrane of some substrate-attached cells. The length of the tethers could reach tens of micrometers and pulled the structures back to the cell when the trap was turned off. We also regarded this event a successful attachment. When crosses were used in these experiments, mostly their flat side touched the cells but successful binding was also observed through the tips of the arms. The drag of the freely-floating cells could then be accomplished with at least 10 μm/s speeds in any lateral direction.

The success rate of cell attachment for the various functionalization combinations can be seen on Table 1. When the streptavidin-coated structures touched the biotinated cells, the success rate was 88.4% for crosses and was 97.5% for ellipsoids; when the cells were not biotinated, this number fell to 30%, showing some unspecific binding of the streptavidin to the cell membrane. When the TPP structures were not coated with the protein, the success rate was always below 10% regardless the cells were biotinated or not.

Table 1. Success rate of the attachment between cells and trapped microstructures

	Biotinated cells		Non-biotinated cells	
Streptavidin-coated crosses	88.4% (97.5% for ellipsoids)	(N = 43)	30%	(N = 20)
Non-coated crosses	7.5%	(N = 53)	2.5%	(N = 40)

3.3 Indirect optical manipulation of cells

From the fact, that the trapped ellipsoids or crosses could not be removed from substrate-attached cells any more, follows that the strength of the binding is higher than the maximum optical force our instrument can exert on them. This is not surprising regarding the rupture force of a single biotin-streptavidin linkage being more than 100 pN [4]. To check the binding during the conditions of manipulation, drag-force experiments were performed when cells indirectly-trapped with functionalized ellipsoids (4 μm short axis, 6 μm long axis) were translated in the medium at controlled speeds. The drag force in the speed range of 10-170 μm/s and for cells of ~20 μm diameter were calculated to be up to 27 pN; at drag speeds higher than about 120-170 μm/s the trap lost the ellipsoid-cell couple. The restoring force acting on the trapped ellipsoids during the drag was independently determined for the speed range where small displacements were measured ($\Delta x < 400$ nm for less than 20 μm/s); for such small displacement the force is still expected to depend linearly on it. The lateral trap stiffness was obtained before the ellipsoid-cell attachment by video-microscopy and was found to be 15 ± 1.5 pN/μm. The histogram of the ellipsoid center position along the x axis before and during a drag of 20 μm/s is shown on Fig. 4(g) displaying a maximum at 400 nm displacement besides the equilibrium positions of no-drag; the corresponding restoring force

#252006 Received 20 Oct 2015; revised 19 Nov 2015; accepted 20 Nov 2015; published 7 Dec 2015

is 6 pN. The viscous force for the same 23 μm diameter cell at 20 μm/s speed is calculated to be 4.3 pN; the drag force for each cell was found to be smaller than the restoring force. One possible reason for the difference is that the ellipsoids and the cells could not be elevated from the substrate surface, which *i)* may impose a friction on the cell during drag and *ii)* should require Faxén's correction in the drag force calculation. Also, the approximation of the ellipsoid-cell couple with a single sphere in the drag force calculation is an underestimation.

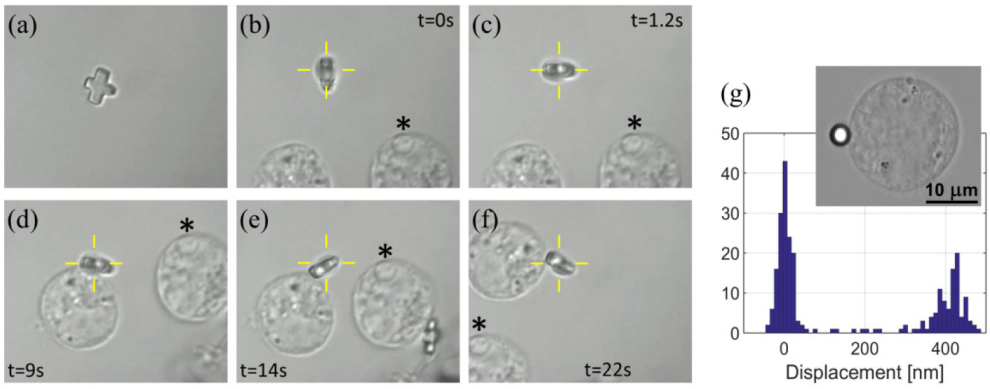

Fig. 4. Indirect optical manipulation of K562 cells (a-f) showing the sequence of the trapping and dragging of a cell with a streptavidin-coated cross (a) (see Visualization 1). The trapped cross is rotated around the optical axis by changing the polarization direction of the trapping beam (b, c). The trapped cross attaches to the cell (d). The cell is dragged around the reference cell marked with asterisk (e, f). Position distribution (g) of the center of an optically trapped ellipsoid dragging a cell; insert: the image of the ellipsoid-cell couple. Crosshairs indicate trap position.

Most importantly regarding the indirect manipulation, we never observed trapped structure-cell detachment during any of the drag experiments. This means that the functionalization provided a reliable protein coating on the TPP structures, and it requires at least 30 pN force to separate them from the cells.

To further demonstrate the applicability of two-photon polymerized structures for indirect cell trapping and manipulation we constructed a complex structure to be used in a multitrap system. The structure that consists of a handle and a probe part is trapped with a set of four static optical traps and can be easily translated in any lateral direction relative to the surrounding medium. According to our knowledge this is the first demonstration of an optically trapped, complex (non-spherical) artificial structure chemically modified in a specific way to actuate a living cell. Figure 5 shows snapshots of translations of the structure with the cell attached to it along all three spatial axes highlighting the effect of the viscous drag (time differences are 1 s in each cases). For the drag along the long axis of the structure (Fig. 5(a)-5(c)) the speed was 19 μm/s, and an average of 420 nm and 500 nm displacement of the rightmost spheroids was observed with the used trapping conditions (Fig. 5(d)); the difference is due to a slight tilt of the structure. During the scan perpendicular to the structure's axis (Fig. 5(e), 5(f)) its tilt was observed and measured to be 4.8 degrees (Fig. 5(g)). The axial drag (along z axis) was carried out by elevating the trapping microscope objective (Fig. 5(h)-5(j)); this kept the trapped structure in focus, while the reference cell on the substrate goes out of focus. The speed of the axial scan was not controlled, but a slight defocus of the indirectly trapped cell was observed during the scan due to the axial viscous drag. Although the manipulations schemes shown here were only translational, it is also possible to rotate these or similar structures with holographic optical tweezers. We aim to explore in a future work that practically any arrangement of trap positions can be updated at high speed with a suitable SLM therefore a carefully designed structure with a cell attached to it can also be rotated to any direction.

#252006 Received 20 Oct 2015; revised 19 Nov 2015; accepted 20 Nov 2015; published 7 Dec 2015

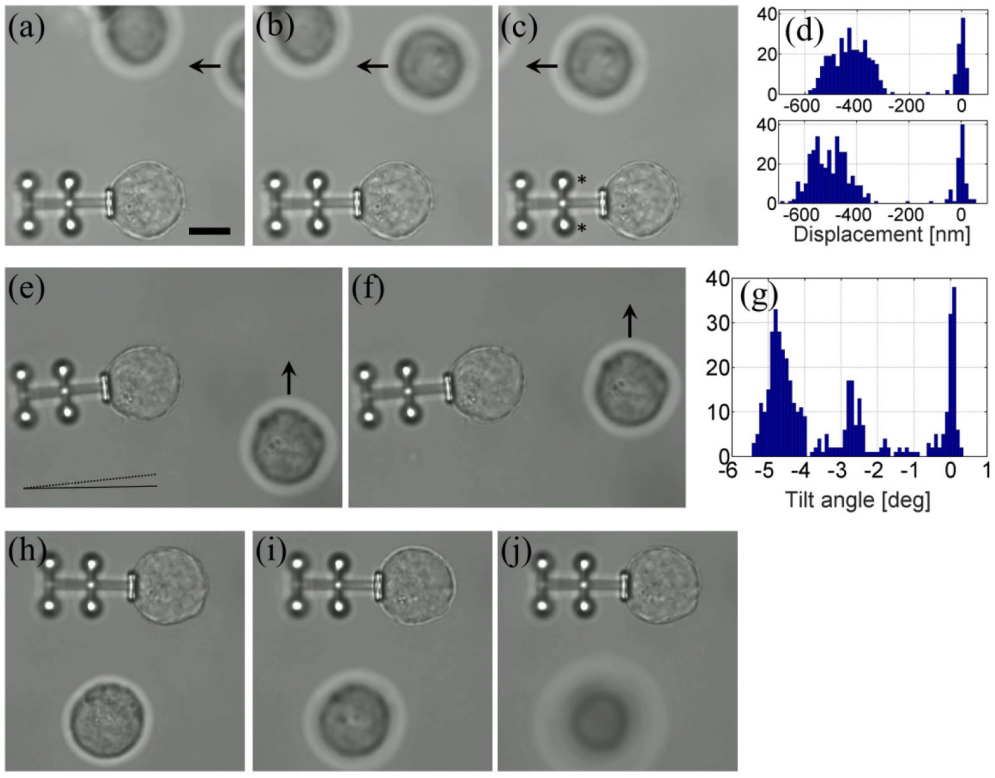

Fig. 5. Translation of an indirectly trapped K562 cell in its medium with a four-spheroid manipulator along the three coordinate axes: (a-c) dragging along the x axis (see Visualization 2), (e)-(f) along the y axis (see Visualization 3) and (h)-(j) along the z (optical) axis. The histograms on panel (d) show the displacement of the two spheroids marked with asterisk during x-drag and that on (g) shows the tilt of the entire structure during y-drag. The two lines on panel (e) indicate the maximum tilt angle. Scale bar: 10 μm.

The analysis of the 3D motion of indirectly manipulated cells with higher precision is the task of the future using more advanced observation schemes; however, it is already apparent from these translation experiments that such trapped cells can be actuated with a rate suitable for most manipulation works. At these speeds the optical trap can still hold the structure-cell couple and their attachment is not compromised either.

4. Conclusion

As the number of applications of indirect optical trapping in biology increases, so does the need to perform experiments overcoming optical damage of cells and for the ability to actuate them with 6 degrees of freedom. We have successfully demonstrated indirect optical manipulation of live cells using complex 3D microtools. By utilizing different PEG-diamine based surface functionalization methods we found that the highest protein surface density is achieved when the protein streptavidin is bound to the SU-8 structures with specific coupling resulting in more than a monolayer of protein on the structure's surface. PEG-diamine linker resulted in about 4 times more surface-bound protein than APTES in our previous study [35]. The attachment success rate between functionalized structures and biotinated cells was at least 90% and the attachment was completed within 2 seconds. Basic indirect optical manipulation of single cells, translations relative to the surrounding medium, was performed with complex structures held by 4 optical traps. We showed that the structure-cell couple can be held stably during translations of reasonable speed along the three spatial coordinates with a small and expectable position change.

#252006 Received 20 Oct 2015; revised 19 Nov 2015; accepted 20 Nov 2015; published 7 Dec 2015

Acknowledgments

The K562 cell line was kindly supported by Dr. Ervin Welker, Institute of Biochemistry, Biological Research Centre. The work was supported by the EU and co-financed by the European Social Fund through the Social Renewal Operational Programme (TÁMOP-4.2.2.D-15/1/KONV-2015-0024) and by the Hungarian Science Research Fund (OTKA grants NN 102624 and NN 114692). This work was supported by funding received from the CONCERT-Japan Photonic Manufacturing Joint Call. L.K. was supported by the Bolyai János Research Scholarship of the Hungarian Academy of Sciences.

#252006 Received 20 Oct 2015; revised 19 Nov 2015; accepted 20 Nov 2015; published 7 Dec 2015